Instituto de Física
Universidade de São Paulo

Constraining the absolute neutrino mass scale and Majorana CP violating phases by future $0\nu\beta\beta$ decay experiments

Nunokawa, H.[1]; Teves, W.J.C.[2] and Zukanovich Funchal, R.[2]

[1]*Instituto de Física Teórica, Universidade Estadual Paulista,*
Rua Pamplona 145, 01405-900 São Paulo, Brazil
[2]*Instituto de Física, Universidade de São Paulo,*
C.P. 66318, 05315-970 São Paulo, Brazil

Publicação IF - 1550/2002

Constraining the absolute neutrino mass scale and Majorana CP violating phases by future $0\nu\beta\beta$ decay experiments

H. Nunokawa[1],* W. J. C. Teves[2],† and R. Zukanovich Funchal[2]‡

[1]*Instituto de Física Teórica, Universidade Estadual Paulista,*

Rua Pamplona 145, 01405-900 São Paulo, Brazil

[2]*Instituto de Física, Universidade de São Paulo C. P. 66.318, 05315-970 São Paulo, Brazil*

Abstract

Assuming that neutrinos are Majorana particles, in a three generation framework, current and future neutrino oscillation experiments can determine six out of the nine parameters which fully describe the structure of the neutrino mass matrix. We try to clarify the interplay among the remaining parameters, the absolute neutrino mass scale and two CP violating Majorana phases, and how they can be accessed by future neutrinoless double beta ($0\nu\beta\beta$) decay experiments, for the normal as well as for the inverted order of the neutrino mass spectrum. Assuming the oscillation parameters to be in the range presently allowed by atmospheric, solar, reactor and accelerator neutrino experiments, we quantitatively estimate the bounds on m_0, the lightest neutrino mass, that can be infered if the next generation $0\nu\beta\beta$ decay experiments can probe the effective Majorana mass (m_{ee}) down to ~ 1 meV. In this context we conclude that in the case neutrinos are Majorana particles: (a) if $m_0 \gtrsim 300$ meV, *i.e.*, within the range directly attainable by future laboratory experiments as well as astrophysical observations, then $m_{ee} \gtrsim 30$ meV must be observed; (b) if $m_0 < 300$ meV, results from future $0\nu\beta\beta$ decay experiments combined with stringent bounds on the neutrino oscillation parameters, specially the solar ones, will place much stronger limits on the allowed values of m_0 than these direct experiments. For instance, if a positive signal is observed around $m_{ee} = 10$ meV, we estimate $3 \lesssim m_0/\text{meV} \lesssim 65$ at 95 % C.L.; on the other hand, if no signal is observed down to $m_{ee} = 10$ meV, then $m_0 \lesssim 55$ meV at 95 % C.L.

PACS numbers: 14.60.Pq, 13.15.+g, 14.60.St

---

*Electronic address: nunokawa@ift.unesp.br

†Electronic address: teves@charme.if.usp.br

‡Electronic address: zukanov@if.usp.br

I. INTRODUCTION

During the last few years, a significant amount of information on the size of the neutrino oscillation parameters have been gathered. Most of what we currently know about these parameters rely on evidences of neutrino flavor transformation that have been collected by the experimental observations of solar [1] as well as of atmospheric neutrinos [2]. The evidences coming from solar neutrino data have been strengthened by the recent neutral current measurement at Sudbury Neutrino Observatory (SNO) [3] whilst those coming from atmospheric neutrinos have also been strongly supported by the K2K accelerator based neutrino oscillation experiment [4]. Furthermore, the negative results of reactor experiments [5] also impose stringent limits on some oscillation parameters.

Assuming that only three active neutrinos participate in oscillations in nature, independent of whether neutrinos are Dirac or Majorana particles, current and future neutrino oscillation experiments can determine at the most six out of the nine parameters which completely describe the neutrino mass matrix, *i.e.*, two mass squared differences (Δm_{12}^2, Δm_{23}^2), three mixing angles (θ_{12}, θ_{13}, θ_{23}) and one CP violating phase (δ) which parametrize the Maki-Nakagawa-Sakata (MNS) [6] leptonic mixing matrix. See, for instance, Refs. [7, 8] for recent discussions on the determination of these *oscillation* parameters.

However, if neutrinos are of the Majorana type, there remain three *non-oscillation* parameters, which can not be accessed by oscillation experiments. They are the absolute neutrino mass scale, which can be taken as the lightest neutrino mass, and two extra CP violating Majorana phases. It is well known that neutrinoless double beta ($0\nu\beta\beta$) decay experiments can shed light on these *non-oscillation* parameters.

The $0\nu\beta\beta$ decay is a process which can occur if and only if neutrinos are Majorana particles [9]. A positive signal of $0\nu\beta\beta$ decay always implies a non-zero electron neutrino mass [10] even if it is not induced by the exchange of a light neutrino but by some other mechanism such as the one in supersymmetry models with broken R-parity [11]. In this work, we assume the simplest possibility to be true, that $0\nu\beta\beta$ decay process is induced only by the exchange of a light neutrino.

It has been abundantly discussed in the literature the relationship between the signals in $0\nu\beta\beta$ decay experiments and oscillation phenomena, see for e.g., Ref. [12]. So far, a large amount of effort has been made to constrain the oscillation parameters from the observation or non-observation of $0\nu\beta\beta$ decay as well as to predict the possible range of the effective

2

Majorana mass in $0\nu\beta\beta$ decay experiments, m_{ee}, from the allowed range of oscillation parameters [12].

In this paper, we take a different point of view. We examine how well we can constrain the three *non-oscillation* parameters by future $0\nu\beta\beta$ decay experiments, considering that the *oscillation* parameters will be soon precisely determined (or constrained) by current and future oscillation experiments. We discuss the interplay among these parameters and the observable signal in future $0\nu\beta\beta$ decay experiments for the normal as well as for the inverted ordering of the neutrino mass spectrum. In particular, presuming the oscillation parameters to be in the range presently allowed by the atmospheric, the solar and the reactor neutrino experiments, we examine what can be concluded about these parameters in the case of either a positive or a negative signal is obtained in future $0\nu\beta\beta$ decay experiments [13].

So far, no convincing signal of $0\nu\beta\beta$ decay has been observed, rather only an upper bound on m_{ee}

$$m_{ee} < 350 \text{ meV}, \tag{1}$$

which comes from the result of the Heidelberg-Moscow Collaboration [14] exists. Recently, an experimental indication of the occurrence of $0\nu\beta\beta$ decay has been announced [15] but since this result seems to be controversial [16], we do not discuss it in this work.

There are many proposals for future $0\nu\beta\beta$ decay experiments to go beyond the bound given in Eq. (1), those include GENIUS [17], CUORE [18], EXO [19], MAJORANA [20] and NOON [21]. It is expected that in the initial phase of the proposed GENIUS experiment [17] the sensitivity to m_{ee} can be as low as ~ 10 meV, going down to ~ 2 meV, if the 10 ton version of the experiment is implemented. In this work, we will try to be optimistic and consider that future experiments will eventually inspect m_{ee} down to ~ 1 meV.

The absolute neutrino mass scale is also independently constrained by the tritium decay experiments, which can directly measure the electron neutrino mass, obtaining the upper bound [22]

$$m_{\nu_e} < 2200 \text{ meV}. \tag{2}$$

The proposed KATRIN experiment aims to stretch the current sensitivity down to ~ 340 meV [23]. We also take this into consideration in our discussions.

This paper is organized as follows. In Sec. II, we describe the theoretical framework on which we base our work. We first discuss in Sec. III, the dependence of the $0\nu\beta\beta$ signal on the lightest neutrino mass, and second in Sec. IV we discuss how the dependence of m_{ee}

on m_0 is related to the two CP phases, α_1 and α_3. In Sec. V we discuss how $m_{ee}^{\min}$, the minimum possible value of m_{ee}, depends on m_0 and θ_{13}. Finally, in Sec. VI, we discuss how the upper as well as the lower bounds on m_0 depend on the solar neutrino oscillation parameters. Sec. VII is devoted to our discussions and conclusions.

II. THE FORMALISM

In this section we discuss the theoretical frame work we will rely upon in this work.

A. Mixing and mass scheme

We consider mixing among three neutrino flavors as,

$$
\begin{bmatrix} \nu_e \\ \nu_\mu \\ \nu_\tau \end{bmatrix} = U \begin{bmatrix} \nu_1 \\ \nu_2 \\ \nu_3 \end{bmatrix}, \tag{3}
$$

where $\nu_\alpha(\alpha = e, \mu, \tau)$ and $\nu_i(i = 1, 2, 3)$ are the weak and the mass eigenstates, respectively, and U is the MNS [6] mixing matrix, which can be parametrized as,

$$
\begin{bmatrix} c_{12}c_{13} & s_{12}c_{13} & s_{13}e^{-i\delta} \\ -s_{12}c_{23} - c_{12}s_{23}s_{13}e^{i\delta} & c_{12}c_{23} - s_{12}s_{23}s_{13}e^{i\delta} & s_{23}c_{13} \\ s_{12}s_{23} - c_{12}c_{23}s_{13}e^{i\delta} & -c_{12}s_{23} - s_{12}c_{23}s_{13}e^{i\delta} & c_{23}c_{13} \end{bmatrix}, \tag{4}
$$

where s_{ij} and c_{ij}, correspond to sine and cosine of $\theta_{i,j}$. We define the neutrino mass-squared differences as $\Delta m_{ij}^2 \equiv m_j^2 - m_i^2$, where $\Delta m_\odot^2 \equiv \Delta m_{12}^2$ is relevant for the solutions to the solar neutrino problem, and $\Delta m_{\mathrm{atm}}^2 \equiv |\Delta m_{23}^2| \simeq |\Delta m_{13}^2|$ is relevant for the atmospheric neutrino observations.

Current atmospheric neutrino data [2] indicate that

$$
\Delta m_{\mathrm{atm}}^2 \equiv |\Delta m_{23}^2| \simeq (2 - 4) \times 10^{-3} \text{ eV}^2, \quad \sin^2 2\theta_{23} \simeq 0.9 - 1, \tag{5}
$$

which combined with nuclear reactor results [5] imply

$$
\sin^2 \theta_{13} \lesssim 0.02, \tag{6}
$$

while the various solar neutrino experiment results strongly suggest that the so called large mixing angle (LMA) MSW solution with parameter in the range [1, 3, 24]

$$
\Delta m_\odot^2 \equiv \Delta m_{12}^2 \simeq (2 - 40) \times 10^{-5} \text{ eV}^2, \quad \tan^2 \theta_{12} \simeq 0.2 - 0.8, \tag{7}
$$

4

will prevail as the explanation to the solar neutrino problem. We will admit throughout this paper that the actual values of these parameters will be confirmed within the above ranges by future neutrino oscillation experiments. Besides further constraining the oscillation parameters given in Eqs. (5)-(7), it is expected that these experiments also can probe the CP violating phase δ and determine the neutrino mass spectrum (sign of Δm_{23}^2) [7].

In this work, we denote the lightest neutrino mass by m_0. Then using $\Delta m_\odot^2$ and Δm_{atm}^2 as defined above, we can describe the two possible mass spectra as follows,

(a) Normal mass ordering:

$$
\begin{aligned}
m_1 &\equiv m_0, \\
m_2 &\equiv \sqrt{m_0^2 + \Delta m_\odot^2}, \\
m_3 &\equiv \sqrt{m_0^2 + \Delta m_\odot^2 + \Delta m_{\text{atm}}^2}.
\end{aligned}
\tag{8}
$$

(b) Inverted mass ordering:

$$
\begin{aligned}
m_1 &\equiv \sqrt{m_0^2 - \Delta m_\odot^2 + \Delta m_{\text{atm}}^2}, \\
m_2 &\equiv \sqrt{m_0^2 + \Delta m_{\text{atm}}^2}, \\
m_3 &\equiv m_0.
\end{aligned}
\tag{9}
$$

In this manner $\Delta m_{12}^2 = \Delta m_\odot^2$ for both mass ordering and $\Delta m_{23}^2 = \pm\Delta m_{\text{atm}}^2$ where the $+(-)$ sign indicates normal (inverted) mass ordering. In Fig. 1, a schematic picture of the mass ordering we consider here is shown.

B. Effective Majorana mass and $0\nu\beta\beta$

Assuming that the $0\nu\beta\beta$ decay process occurs through the exchange of a light ($m_\nu < 10$ MeV) neutrino, the theoretically expected half-life of the $0\nu\beta\beta$ decay, $T_{1/2}^{0\nu}$, is given by [25],

$$
[T_{1/2}^{0\nu}]^{-1} = G^{0\nu}|M_{0\nu}|^2 m_{ee}^2,
\tag{10}
$$

where $G^{0\nu}$ denotes the exact calculable phase space integral, $M_{0\nu}$ consist of the sum of the Gamow-Teller and the Fermi nuclear matrix elements defined as in Ref. [25] and m_{ee} is the effective Majorana mass defined in Eq. (11) below.

It is known that the evaluation of the nuclear matrix elements suffers from a large uncertainty depending on the adopted method used in the calculations. As we can see in Table

I of Ref. [25], the evaluated half-lives for a given nucleus and a given value of m_{ee} typically vary within a factor of ~ 10. This implies a factor of ~ 3 uncertainty in m_{ee} when extracting it from the results of $0\nu\beta\beta$ decay experiments, which in fact directly measure or constrain not m_{ee} but the value of $T_{1/2}^{0\nu}$.

The effective Majorana mass, m_{ee}, is given by,

$$
\begin{aligned}
m_{ee} &= |m_1 U_{e1}^2 + m_2 U_{e2}^2 + m_3 U_{e3}^2|, \\
&= |m_1 c_{12}^2 c_{13}^2 e^{2i\alpha_1} + m_2 s_{12}^2 c_{13}^2 + m_3 s_{13}^2 e^{2i\alpha_3}|,
\end{aligned}
\tag{11}
$$

where we have chosen to attach the CP violating phases to the first and third elements. Note that α_1 and α_3 must be understood as the relative phases of U_{e1} and U_{e3} with respect to that of U_{e2}. The range of these phases are

$$
0 \leq \alpha_1 \leq \pi, \quad 0 \leq \alpha_3 \leq \pi.
\tag{12}
$$

As it is known, the value of m_{ee} can be perceived as the norm of the sum of three vectors $\vec{m}_{ee}^{(1)}$, $\vec{m}_{ee}^{(2)}$ and $\vec{m}_{ee}^{(3)}$ in the complex plane whose absolute values are given by,

$$
\begin{aligned}
m_{ee}^{(1)} &\equiv |\vec{m}_{ee}^{(1)}| \equiv |U_{e1}^2| m_1 = m_1 c_{12}^2 c_{13}^2, \\
m_{ee}^{(2)} &\equiv |\vec{m}_{ee}^{(2)}| \equiv |U_{e2}^2| m_2 = m_2 s_{12}^2 c_{13}^2, \\
m_{ee}^{(3)} &\equiv |\vec{m}_{ee}^{(3)}| \equiv |U_{e3}^2| m_3 = m_3 s_{13}^2.
\end{aligned}
\tag{13}
$$

Explicitly, m_{ee} is expressed as

$$
\begin{aligned}
m_{ee}^2 &= [m_{ee}^{(1)} \cos 2\alpha_1 + m_{ee}^{(2)} + m_{ee}^{(3)} \cos 2\alpha_3]^2 + [m_{ee}^{(1)} \sin 2\alpha_1 + m_{ee}^{(3)} \sin 2\alpha_3]^2, \\
&= [m_{ee}^{(1)}]^2 + [m_{ee}^{(2)}]^2 + [m_{ee}^{(3)}]^2 + 2\{ m_{ee}^{(1)} m_{ee}^{(2)} \cos 2\alpha_1 \\
&\quad + m_{ee}^{(2)} m_{ee}^{(3)} \cos 2\alpha_3 + m_{ee}^{(1)} m_{ee}^{(3)} \cos[2(\alpha_1 - \alpha_3)] \}, \\
&= m_1^2 c_{12}^4 c_{13}^4 + m_2^2 s_{12}^4 c_{13}^4 + m_3^2 s_{13}^4 + 2\{ m_1 m_2 c_{12}^2 s_{12}^2 c_{13}^4 \cos 2\alpha_1 \\
&\quad + m_2 m_3 s_{12}^2 c_{13}^2 s_{13}^2 \cos 2\alpha_3 + m_1 m_3 c_{12}^2 c_{13}^2 s_{13}^2 \cos[2(\alpha_1 - \alpha_3)] \}.
\end{aligned}
\tag{14}
$$

We can clearly see from Eq. (14) that m_{ee} is invariant under the transformation

$$
(\alpha_1, \alpha_3) \to (\pi - \alpha_1, \pi - \alpha_3),
\tag{15}
$$

which allows us to further restrict the range of (α_1, α_3), without loss of generality, to

$$
0 \leq \alpha_1 \leq \pi, \quad 0 \leq \alpha_3 \leq \pi/2.
\tag{16}
$$

6

We note that α_1 and/or α_3 different from 0 and $\pi/2$ imply CP violation.

The maximum possible value of m_{ee}, denoted by $m_{ee}^{\max}$, is given by,

$$
\begin{aligned}
m_{ee}^{\max} &= m_{ee}^{(1)} + m_{ee}^{(2)} + m_{ee}^{(3)}, \\
&= (m_1 c_{12}^2 + m_2 s_{12}^2) c_{13}^2 + m_3 s_{13}^2.
\end{aligned}
\tag{17}
$$

which occurs for $\alpha_1 = \alpha_3 = 0$. On the other hand, the minimum possible value of m_{ee} is zero only when the three vectors $\vec{m}_{ee}^{(i)}$ $(i = 1, 2, 3)$ can form a triangle. This can occur when the condition,

$$
m_{ee}^{(i)} < \sum_{j \neq i} m_{ee}^{(j)} \quad (i = 1, 2, 3),
\tag{18}
$$

is satisfied. When these three vectors can not form a closed triangle, which includes the case when one of them is null, the minimum value is given by twice the length of the largest vector minus the sum of the norm of all three vectors,

$$
m_{ee}^{\min} = 2 \max\{m_{ee}^{(1)}, m_{ee}^{(2)}, m_{ee}^{(3)}\} - [m_{ee}^{(1)} + m_{ee}^{(2)} + m_{ee}^{(3)}].
\tag{19}
$$

The values of (α_1, α_3) which lead to such a minimum are $(\alpha_1, \alpha_3) = (\pi/2, 0)$, $(\pi/2, \pi/2)$ or $(0, \pi/2)$ when respectively $m_{ee}^{(1)}$, $m_{ee}^{(2)}$ or $m_{ee}^{(3)}$ is the largest contribution.

C.   Some useful extreme limits

To help the comprehension of our discussions in the following sections, let us review here the approximated expressions for $m_{ee}^{\max}$ and $m_{ee}^{\min}$ for the two extreme cases of the absolute neutrino mass scale: vanishing m_0 and very large m_0 compared to $\sqrt{\Delta m_{\mathrm{atm}}^2}$. The neutrino oscillation parameters are assumed to lie in the ranges given in Eqs. (5)-(7).

(i) Vanishing m_0 limit:

For the normal mass ordering we have,

$$
m_{ee}^{\min}, m_{ee}^{\max} \simeq m_{ee}^{(2)} \mp m_{ee}^{(3)} \simeq \sqrt{\Delta m_{\odot}^2} s_{12}^2 c_{13}^2 \mp \sqrt{\Delta m_{\mathrm{atm}}^2} s_{13}^2,
\tag{20}
$$

where the $-(+)$ sign corresponds to $m_{ee}^{\min}$ ($m_{ee}^{\max}$).

For the inverted mass ordering we have,

$$
m_{ee}^{\min} \simeq m_{ee}^{(1)} - m_{ee}^{(2)} \simeq \sqrt{\Delta m_{\mathrm{atm}}^2} \cos 2\theta_{12} c_{13}^2,
\tag{21}
$$

$$
m_{ee}^{\max} \simeq m_{ee}^{(1)} + m_{ee}^{(2)} \simeq \sqrt{\Delta m_{\mathrm{atm}}^2} c_{13}^2.
\tag{22}
$$

(ii) Large m_0 ($\gg \sqrt{\Delta m_{\text{atm}}^2}$) limit:

For the normal as well as for the inverted mass ordering,

$$m_{ee}^{\min} \simeq m_{ee}^{(1)} - m_{ee}^{(2)} - m_{ee}^{(3)} \simeq m_0(c_{13}^2 \cos 2\theta_{12} - s_{13}^2), \tag{23}$$

$$m_{ee}^{\max} \simeq m_{ee}^{(1)} + m_{ee}^{(2)} + m_{ee}^{(3)} \simeq m_0. \tag{24}$$

III. DEPENDENCE ON THE LIGHTEST NEUTRINO MASS

In this section we examine how the effective Majorana mass, m_{ee}, depends on the lightest neutrino mass, m_0, and clarify the importance of each of the individual contributions, $m_{ee}^{(1)}$, $m_{ee}^{(2)}$ and $m_{ee}^{(3)}$ to m_{ee}. We present in Fig. 2 for normal (upper panels) as well as inverted (lower panels) mass ordering, the maximum and minimum values of m_{ee} as a function of m_0 for vanishing θ_{13} (left panels) and $\sin^2 \theta_{13} = 0.02$ (right panels). In the same plots we also show the individual contributions of $m_{ee}^{(1)}$, $m_{ee}^{(2)}$ and $m_{ee}^{(3)}$ by dashed, dotted and dash-dotted lines, respectively.

Let us first discuss the case of normal mass ordering. As we can see from the plots in the upper panels of Fig. 2, for smaller values of m_0, $m_{ee}^{(2)}$ is the dominant contribution whereas for larger values of m_0, $m_{ee}^{(1)}$ dominates over the other contributions. For the typical values of the oscillation parameters allowed by the solar, atmospheric neutrino and reactor data, $m_{ee}^{(3)}$ is almost always the smallest contribution to m_{ee}, being subdominant in m_{ee} and it can only be important when there is a large cancellation between $m_{ee}^{(1)}$ and $m_{ee}^{(2)}$.

It is clear that a strong cancellation in m_{ee} can occur if at least two of $m_{ee}^{(1)}$, $m_{ee}^{(2)}$ and $m_{ee}^{(3)}$ are comparable in magnitude. Just by comparing their magnitudes in the plots in Fig. 2, we can easily see for which values of m_0 a strong cancellation in m_{ee} can occur. For the case if $\theta_{13} = 0$, m_{ee} can be zero only at one particular value of m_0 (see Fig. 2 (a)) whereas for the case if $\theta_{13} \neq 0$ m_{ee} can be zero for some range of m_0 (see Fig. 2(b)). See Sec. V for more detailed discussions about the dependence of $m_{ee}^{\min}$ on m_0 and θ_{13}.

In the case of inverted mass ordering, the situation changes significantly. Here $m_{ee}^{(1)} > m_{ee}^{(2)} >> m_{ee}^{(3)}$ and $m_{ee}^{\min} \neq 0$ always must satisfy the condition,

$$m_{ee}^{\min} \gtrsim \sqrt{\Delta m_{\text{atm}}^2} \cos 2\theta_{12} \sim 10 \ \text{meV}, \tag{25}$$

for any value of m_0 for current allowed parameters from solar and atmospheric neutrino data and no complete cancellation in m_{ee} is expected as we can see clearly from the plots in the

lower panels of Fig. 2. Therefore, if no positive signal of $0\nu\beta\beta$ is observed down to ~ 10 meV, inverted mass ordering can be excluded as long as neutrinos are Majorana particles.

IV. DEPENDENCE ON THE LIGHTEST NEUTRINO MASS AND CP PHASES

Let us next discuss how the m_{ee} dependence on m_0 is related to the two CP phases, α_1 and α_3. We present in Fig. 3 iso-contour plots of m_{ee} in the m_0-α_1 plane for vanishing θ_{13}, for the normal mass ordering, for some values of the solar parameters taken within the allowed ranges given in Eq. (7). Note that, in this particular case, there is no dependence on the phase α_3 in our choice of parametrization, which is clear from Eq. (11).

Fist we note that in the plots, iso-contours are symmetric with respect to $\alpha_1/\pi = 0.5$. Second we note that if m_{ee} is smaller than certain value, m_{ee}^{crit}, the iso-contours are closed which means that the possible values of both m_0 and α_1 are bounded to some limited range, which does not include zero. The critical value of m_{ee} under which the contour is a closed one is given by

$$m_{ee}^{\mathrm{crit}} \simeq m_{ee}^{(2)} = \sqrt{\Delta m_\odot^2} s_{12}^2 \simeq (1 - 10) \text{ meV}, \tag{26}$$

this dependence is illustrated in Fig. 3. If a positive $0\nu\beta\beta$ signal is not observed down to these values, this will imply either that m_0 as well as the CP phase α_1 are bounded to the limited range within the closed contours shown in Fig. 3 or that neutrinos are of not Majorana type particles.

We show in Fig. 4 the same information as in Fig. 3(b) but for $\sin^2\theta_{13} = 0.01$ (left panels) and 0.02 (right panels) for three different values of $\alpha_3 = 0, \pi/4$ and $\pi/2$ in the upper, middle and lower panels, respectively. As we can see from these plots the qualitative behaviors of the contours are very similar to those in Fig. 3(b). This is due to the fact that $m_{ee}^{(3)}$, which is the only term that carries the contributions of $\sin^2\theta_{13}$ and α_3, is subdominant compared to the other two elements in m_{ee}. The effect of a non-zero α_3 is to cause some displacement of the position of the symmetry line of the plots from around $\alpha_1/\pi = 0.5$ to somewhat smaller values.

Let us here mention the case where m_0 can be independently measured by another experiment such as the KATRIN [23] tritium decay one. In this case, it is possible to constrain the CP phase α_1 by comparing the measured values of m_{ee} and m_0 provided that $m_0 \gtrsim 340$ meV, the maximum sensitivity of KATRIN. If a $0\nu\beta\beta$ decay experiment measures m_{ee} significantly smaller than m_0 measured by KATRIN, this would imply a non-zero CP phase

α_1. This is because for the m_0 values relevant for KATRIN, $m_{ee} \sim m_0$ if $\alpha_1 \simeq 0$, but m_{ee} can be as small as $\sim 0.1 \times m_0$ if $\alpha_1 \sim \pi/2$ and if the largest allowed value of θ_{12} from the current LMA allowed region is realized (see Eqs. (23) and (24)). However, it would still be difficult to say something definite about the value of α_1 for $10 \lesssim m_0/\text{meV} \lesssim 340$.

Our plots in Figs. 3 and 4 are in agreement with the conclusion presented in Ref. [26], that is, either a positive or a negative results in a $0\nu\beta\beta$ decay experiment can constrain m_0 and α_1 but, since the possible values of α_1 will always include $\pi/2$, a non-zero value of α_1 cannot be interpreted as an evidence of CP violation, even if a positive signal of $0\nu\beta\beta$ decay is observed. Unfortunately, to be able to say anything more definite on the CP phase, independent precise information on m_0 is unavoidable. Moreover, nothing can be concluded about the value of α_3.

We show in Fig. 5 the same information as in Fig. 3 for the inverted mass ordering. Since there is no significant dependence on θ_{13} or on α_3 in this case, we show only the curves for vanishing θ_{13}. We note from these plots that there is no lower bound for m_0 as long as $m_{ee} \lesssim 50$ meV, and moreover, α_1 is less constrained if compared to the case of normal ordering, independently of the values of the other neutrino oscillation parameters.

V. DEPENDENCE ON THE LIGHTEST NEUTRINO MASS AND θ_{13}

In this and the next sections we focus on the relation among m_{ee} and some of the yet undetermined mixing parameters. Let us start by discussing the dependence of m_{ee}^{min} on m_0 and θ_{13}. Here we discuss only the case of normal ordering since the dependence on θ_{13} for the inverted case is quite small. We present in Fig. 6, the iso-contour plots of m_{ee}^{min} in the s_{13}^2-m_0 plane for some different choices of the oscillation parameters.

For vanishing θ_{13}, one can have $m_{ee}^{\text{min}} = 0$ if $m_{ee}^{(1)} = m_{ee}^{(2)}$, i.e. , $m_1 c_{12}^2 = m_2 s_{12}^2$, which is equivalent to,

$$m_0 = \frac{s_{12}^2}{\sqrt{|\cos 2\theta_{12}|}} \sqrt{\Delta m_\odot^2} \sim 3 \text{ meV},\tag{27}$$

where we have computed the numerical estimate using the best fitted values of the parameters from the latest solar neutrino data (see Fig. 2(a) and Fig. 6(b)). Within the current allowed range given in Eq. (7), the possible values of m_0 for which we can expect strong cancellation are in the range $m_0 \simeq (0.9 - 12)$ meV, as we can confirm with the plots in Fig. 6.

For non-zero values of θ_{13}, as we can see clearly from Fig. 6, $m_{ee}^{\min}$ can take zero for some range of m_0. We can also see that there is a critical value of θ_{13} for which $m_{ee}^{\min}$ is zero with vanishing m_0. Such a value of θ_{13} can be easily estimated by solving $m_2 c_{13}^2 s_{12}^2 = m_3 s_{13}^2$ with $m_0 \to 0$ which is equivalent to,

$$s_{13}^2 \simeq \sqrt{\frac{\Delta m_\odot^2}{\Delta m_{\text{atm}}^2}} s_{12}^2 \sim 0.03, \tag{28}$$

for the best fitted parameters from solar as well as atmospheric neutrino data. We note that this is close to the current upper bound on s_{13}^2 allowed by the CHOOZ result [5]. Letting $\Delta m_\odot^2$, Δm_{atm}^2 and s_{12}^2 take any value in the region consistent with the solar and atmospheric neutrino observations given in Eq. (5) and (7), the range of s_{13}^2 for which strong cancellation can occur is $s_{13}^2 \simeq 0.01 - 0.20$, which is again consistent with our results in Fig. 6.

We observe that if s_{13}^2 is smaller than the critical value given in Eq. (28), the value of m_0 can be strongly constrained to some limited range around the value of m_0 given in Eq. (27), provided that future $0\nu\beta\beta$ experiment can probe a m_{ee} value as small as $\sim \sqrt{\Delta m_\odot^2 s_{12}^2}$ independent of whether a positive or negative signal of $0\nu\beta\beta$ is observed.

VI.   CONSTRAINING m_0 USING SOLAR NEUTRINO DATA

Finally, let us discuss how we can constrain m_0 using the solar neutrino parameters. Let us first analyze the case where a positive signal of $0\nu\beta\beta$ is observed. The value of m_{ee} has to be extracted from the experimental measured half-life, $T_{1/2}^{0\nu}$, of the decaying parent nucleus by comparison with the theoretical prediction which rely on nuclear matrix element calculations. As mentioned in Sec. II B, typically, there is a factor three difference among the results of the matrix element evaluations according to different model assumptions [25]. In order to take such uncertainty into account we will consider here a somewhat optimistic, but reasonable assumption, of 30% uncertainty on the determination of m_{ee} by future $0\nu\beta\beta$ experiments. Hopefully improvements on the understanding of the underlining nuclear physics effects can decrease this uncertainty even further.

In Fig. 7 we show the iso-contours of upper ($m_0^{\max}$) and lower ($m_0^{\min}$) bounds on m_0 in units of meV in the $\tan^2 \theta_{12}$-Δm_{12}^2 plane for the case where a positive signal of $0\nu\beta\beta$ is observed with central values m_{ee} = 10, 5, 3 and 1 meV with a 30 % uncertainty. In these plots we have used $\Delta m_{23}^2 = 3 \times 10^{-3}$ eV^2 and $\sin^2 \theta_{13} = 0$. We do not present plots for

$m_{ee} > 10$ meV, since in these cases the upper and lower bound can be analytically estimated as we will see below.

When $m_0 > \sqrt{\Delta m^2_{\rm atm}}$ the upper bound on m_0 does not depend much on $\Delta m^2_\odot$ but essentially only on θ_{12} (see Eq. (23) in Sec. II C), it is given as,

$$m_0^{\rm max} \sim \frac{m_{ee}}{\cos 2\theta_{12}}, \tag{29}$$

and the lower bound $m_0^{\rm min} \sim m_{ee}$, independent of the solar parameters in the region compatible with the LMA MSW solution to the solar neutrino problem.

We observe that, as can be seen in Fig. 7, that as m_{ee} decreases, the upper bound lines, which mainly depend on $\tan^2 \theta_{12}$, are shifted to larger values of θ_{12}, decreasing $m_0^{\rm max}$ for a given set of $(\tan^2 \theta_{12}, \Delta m^2_{12})$. The lower bound lines, on the other hand, depend more on Δm^2_{12} and there are some regions where no lower bound is obtained. For $m_{ee} \gtrsim 10$ meV or $m_{ee} \lesssim 1$ meV there is always a lower bound found inside the currently allowed LMA MSW region, whereas for $1 \lesssim m_{ee}/{\rm meV} \lesssim 10$ this is not true. The appearance of these no lower bound bands comes from the fact the in these regions the solar mass scale alone is sufficient to explain the positive signal observed, even for vanishing m_0.

In Fig. 8 we repeat the same exercise but for $\sin^2 \theta_{13} = 0.02$. The most significant effect of a non zero $\sin^2 \theta_{13}$ is the increase of the size of the no lower bound band, which can in some cases stretch over the entire LMA allowed region, otherwise the behavior of the upper and lower bound lines is qualitatively similar to the previous case.

Let us next consider the case where no positive signal is observed. In Fig. 9 we present the same information as in Fig. 7 but for the case where no positive signal of $0\nu\beta\beta$ is observed down to $m_{ee} = 10$ meV (a), 5 meV (b), 3 meV (c) and 1 meV (d). We can see that qualitative behavior of the iso-contours for the upper bound is similar to that in Fig. 7 but it is different for the trend of the lower bound curves. Compared to the case where positive $0\nu\beta\beta$ signal is obtained, it is more difficult to put lower bound on m_0. This can be easily understood from Fig. 2 (a). We note that unless we can constrain m_{ee} down to ~ 3 meV, no lower bound on m_0 is obtained. In Fig. 10 we present the same information as in Fig. 9 but for $\sin^2 \theta_{13} = 0.02$. Again, the qualitative behavior of the iso-contours is similar to the case of $\sin^2 \theta_{13} = 0$. The difference from the previous case presented in Fig. 9 is that the constraint on m_0 become somewhat weaker, leading to larger upper bounds and smaller lower bounds for a given set of $(\tan^2 \theta_{12}, \Delta m^2_{12})$.

Finally, let us also comment the case of inverted ordering. For this case, we can easily

estimate the upper as well as lower bound from the analytic expressions as well as from the lower panels of Fig. 2. Let us look at Fig. 2 (c) and (d). First of all, if the inverted ordering is the case, the observed value of m_{ee} in $0\nu\beta\beta$ decay experiment must be larger than the value given in Eq. (25), as already mentioned in Sec. III. If the observed m_{ee} is smaller than $\sqrt{\Delta m^2_{\mathrm{atm}}c^2_{13}}$ (see Eq. (22)) then there is no lower bound on m_0 whereas the upper bound is given by the same expression for the case of normal ordering, by Eq. (29). If the observed m_{ee} value is larger than $\sqrt{\Delta m^2_{\mathrm{atm}}c^2_{13}}$, then the upper as well as lower bounds are given by the same expression as in the case of normal ordering, which is already discussed in this section.

VII. DISCUSSIONS AND CONCLUSIONS

We have studied how the *non-oscillation* neutrino parameters which can not be extracted from the oscillation analysis, the absolute neutrino mass scale and two CP violating Majorana phases, can be accessed by the positive or negative signal of future $0\nu\beta\beta$ decay experiments. We have carried out this by choosing various different set of mixing parameters which are varied within the parameter region currently allowed by the solar, atmospheric as well as by reactor neutrino experiments.

In the future, the KATRIN experiment expects to directly inspect m_0 down to ~ 340 meV [23], while there are several proposed astrophysical measurements on the temperature perturbation in the early universe imprinted in the cosmic microwave background radiation, such as the ones that can be performed by MAP (Microwave Anisotropy Probe) [28] and Planck [29], which can probe m_0 down to ~ 300 meV [30], where the expected sensitivity suffers from the uncertainty coming from cosmological parameters. It is expected that future supernova neutrino measurements can probe m_0 down to at most $\sim$ (2-3) eV [31].

Our analysis permit us to conclude that if these experiments measure $m_0 \gtrsim 300$ meV, then either a positive signal of $0\nu\beta\beta$ decay compatible with $m_{ee} \gtrsim 30$ meV must be observed in the near future or neutrinos are Dirac particles. This is simply because $m^{\mathrm{min}}_{ee} \sim m_0 \cos 2\theta_{12}$ (see Eq. (23) in Sec. II C) and $\cos 2\theta_{12} \gtrsim 0.1$ from the current allowed LMA parameter region given in Eq. (7).

On the other hand, if these experiments do not observe any positive signal of $m_0 \gtrsim 300$ meV, results from future $0\nu\beta\beta$ decay experiments combined with more precise values of the neutrino oscillation parameters, specially the solar ones (Δm^2_{12}, $\tan^2 \theta_{12}$), which can be

13

precisely determined by the KamLAND experiment [8], will place more stringent bounds on m_0 for the Majorana case provided that the sensitivity of $m_{ee} \lesssim 30$ meV is achieved. To be more specific, if a positive signal is observed around $m_{ee} = 10$ meV (assuming a 30% uncertainty on the determination of m_{ee}), we estimate $3 \lesssim m_0/\text{meV} \lesssim 65$ at 95 % C.L.; on the other hand, if no signal is observed down to $m_{ee} = 10$ meV, then $m_0 \lesssim 55$ meV at 95 % C.L. Allowing for a more optimistic sensitivity, a positive signal observed around $m_{ee} = 3$ meV or no signal seen down to 3 meV would mean $m_0 \lesssim 25$ meV at 95 % C.L. These bounds can be improved by a better determination of $\tan^2 \theta_{12}$, Δm_{12}^2 and $\sin^2 \theta_{13}$ as can be clearly seen in Figs. 7- 10, as well as by the reduction of the uncertainties in the theoretical calculations of the nuclear matrix elements.

We finally conclude that it is possible to constrain the CP violating phase α_1 to values around $\pi/2$ if: (1) m_0 is large enough to be detected by KATRIN or by astrophysical observations and future $0\nu\beta\beta$ decay experiments observe m_{ee} close to its minimum value or (2) future $0\nu\beta\beta$ decay experiments can achieve a sensitivity on $m_{ee} \lesssim 10$ meV, independently of whether a positive or a negative signal is observed. Unfortunately, nothing can be known about α_3.

Acknowledgments

[1] Q. R. Ahmad et al. (SNO Collaboration), Phys. Rev. Lett. **87**, 071301 (2001); S. Fukuda et al. (Super-Kamiokande Collaboration), Phys. Rev. Lett. **86**, 5651 (2001); ibid. **86**, 5656 (2001); arXiv:hep-ex/0205075; K. Lande et al. (Homestake Collaboration), Astrophys .J. **496**, 505 (1998); J. Abdurashitov et al. (SAGE Collaboration), Phys. Rev. C **60**, 055801 (1999); W. Hampel et al. (GALLEX Collaboration), Phys. Lett. B **447**, 127 (1999); M. Altmann et al. (GNO Collaboration), Phys. Lett. B **490**, 16 (2000).

[2] Y. Fukuda et al. (Super-Kamiokande Collaboration), Phys. Rev. Lett. **81**, 1562 (1998); H. S. Hirata et al. (Kamiokande Collaboration), Phys. Lett. B **205**, 416 (1988); ibid. **280**, 146

(1992); Y. Fukuda *et al.*, *ibid.* **335**, 237 (1994); R. Becker-Szendy *et al.* (IMB Collaboration), Phys. Rev. D **46**, 3720 (1992); M. Ambrosio *et al.* (MACRO Collaboration), Phys. Lett. B **478**, 5 (2000); B. C. Barish, Nucl. Phys. B (Proc. Suppl.) **91**, 141 (2001); W. W. M. Allison *et al.* (Soudan-2 Collaboration), Phys. Lett. B **391**, 491 (1997); Phys. Lett. B **449**, 137 (1999); W. A. Mann, Nucl. Phys. B (Proc. Suppl.) **91**, 134 (2001);

[3] Q. R. Ahmad *et al.* (SNO Collaboration), arXiv:nucl-ex/0204008, arXiv:nucl-ex/0204009.

[4] S. H. Ahn *et al.* (K2K Collaboration), Phys. Lett. B **511**, 178 (2001); J. E. Hill (K2K Collaboration), in *Proc. of the APS/DPF/DPB Summer Study on the Future of Particle Physics (Snowmass 2001)* ed. by R. Davidson and C. Quigg, arXiv:hep-ex/0110034.

[5] M. Apollonio *et al.* (CHOOZ Collaboration), Phys. Lett. B **420**, 397 (1998); *ibid.* **466**, 415 (1999); F. Boehm *et al.* (Palo Verde Collaboration), Phys. Rev. D **62**, 072002 (2000); Phys. Rev. D **64**, 112001 (2001).

[6] Z. Maki, M. Nakagawa, and S. Sakata, Prog. Theor. Phys. **28**, 870 (1962).

[7] H. Minakata and H. Nunokawa, JHEP **0110**, 001 (2001), V. Barger *et al.*, Phys. Rev. D **65**, 053016 (2002); T. Kajita, H. Minakata and H. Nunokawa, Phys. Lett. B **528**, 245 (2002); M. Aoki *et al.*, arXiv:hep-ph/0112338; P. Huber, M. Lindner and W. Winter, arXiv:hep-ph/0204325; A. Donini, D. Meloni and P. Migliozzi, arXiv:hep-ph/0206034; V. Barger, D. Marfatia and K. Whisnant, arXiv:hep-ph/0206038; G. Barenboim *et al.*, arXiv:hep-ph/0204208; arXiv:hep-ph/0206025.

[8] V. Barger, D. Marfatia and B. P. Wood, Phys. Lett. B **498**, 53 (2001); H. Murayama and A. Pierce, Phys. Rev. D **65**, 013012 (2002); A. de Gouvea and C. Pena-Garay, Phys. Rev. D **65**, 0113011 (2001); M. C. Gonzalez-Garcia and C. Pena-Garay, Phys. Lett. B **527**, 199 (2002); P. Aliani *et al.*, arXiv:hep-ph/0205061.

[9] M. Doi, T. Kotani and E. Takasugi, Prog. Theor. Phys. Suppl. **83**, 1 (1985); T. Tomoda, Rep. Prog. Phys. **54**, 53 (1991).

[10] J. Schechter and J. W. F. Valle, Phys. Rev. D **25**, 2951 (1982).

[11] M. Hirsch, H. V. Klapdor-Kleingrothaus and S. G. Kovalenko, Phys. Rev. Lett. **75**, 17 (1995); Phys. Rev. D **53**, 1329 (1996); M. Hirsch and J. W. F. Valle, Nucl. Phys. B **557**, 60 (1999).

[12] S. T. Petcov and A. Yu. Smirnov, Phys. Lett. B **322**, 109 (1994); H. Minakata and O. Yasuda, Phys. Rev. D **56**, 1692 (1997); H. Minakata and O. Yasuda, Nucl. Phys. B **523**, 597 (1998); T. Fukuyama, K. Matsuda and H. Nishiura, Phys. Rev. D **57**, 5844 (1998); *ibid.* **81**, 4279

(1998); F. Vissani, JHEP **9906**, 022 (1999); S. M. Bilenkii *et al.*, Phys. Lett. B **465**, 193 (1999); K. Matsuda *et al.*, Phys. Rev. D **62**, 093001 (2000); H. V. Klapdor-Kleingrothaus, H. Päs and A. Yu. Smirnov, Phys. Rev. D **63**, 073005 (2001); W. Rodejohann, Nucl. Phys. B **597**, 110 (2001); Y. Farzan, O. L. G. Peres and A. Yu. Smirnov, Nucl. Phys. B **612**, 59 (2001); S. M. Bilenky, S. Pascoli and S. T. Petcov, Phys. Rev. D **64**, 053010 (2001); H. Minakata and H. Sugiyama, Phys. Lett. B **526**, 335 (2002); *ibid.* **532**, 275 (2002); W. Rodejohann, arXiv:hep-ph/0203214; F. Feruglio, A. Strumia and F. Vissani, arXiv:hep-ph/0201291, to appear in Nucl. Phys. B; S. Pascoli and S. T. Petcov, arXiv:hep-ph/0205022.

[13] For instance, the following articles also discussed and demonstrated the relation between $0\nu\beta\beta$ decay signal and the absolute neutrino mass scales and/or Majorana CP phases but in different ways from the ones we consider in this work: V. Barger and K. Whisnant, Phys. Lett. B **456**, 194 (1999); H. Päs and T. J. Weiler, Phys. Rev. D **63**, 113015 (2001); P. Osland and G. Vigdel, Phys. Lett. B **520**, 143 (2001); V. Barger *et al.*, Phys. Lett. B **532**, 15 (2002); M. Frigerio and A. Yu. Smirnov, arXiv:hep-ph/0202247.

[14] H. V. Klapdor-Kleingrothaus *et al.* (Heidelberg–Moscow Collaboration), Eur. Phys. J. A **12**, 147 (2001); see also C. E. Aalseth *et al.* (16EX Collaboration), arXiv:hep-ex/0202026.

[15] H. V. Klapdor-Kleingrothaus *et al.*, Mod. Phys. Lett. A **16**, 2409 (2001).

[16] C. E. Aalseth *et al.*, arXiv:hep-ex/0202018; H. V. Klapdor-Kleingrothaus, arXiv:hep-ph/0205288; H. L. Harney, arXiv:hep-ph/0205293.

[17] H. V. Klapdor-Kleingrothaus *et al.* (GENIUS Collaboration), arXiv:hep-ph/9910205.

[18] E. Fiorini *et al.*, Phys. Rep. **307**, 309 (1998); A. Bettini, Nucl. Phys. Proc. Suppl. **100**, 332 (2001).

[19] M. Danilov *et al.*, Phys. Lett. B **480**, 12 (2000).

[20] C. E. Aalseth *et al.* (MAJORANA Collaboration), arXiv:hep-ex/0201021.

[21] H. Ejiri *et al.*, Phys. Rev. Lett. **85**, 2917 (2000).

[22] J. Bonn *et al.*, (Mainz Collaboration), Nucl. Phys. Proc. Suppl. **91**, 273 (2001).

[23] A. Osipowicz *et al.* (KATRIN Collaboration), arXiv:hep-ex/0109033.

[24] G. L. Fogli *et al.*, Phys. Rev. D **64**, 093007 (2001); A. M. Gago *et al.*, Phys. Rev. D **65**, 073012 (2002); J. N. Bahcall *et al.*, arXiv:hep-ph/0204314; A. Bandyopadhyay *et al.*, arXiv:hep-ph/0204286 V. Barger *et al.*, arXiv:hep-ph/0204253; P. C. de Holanda and A. Yu. Smirnov arXiv:hep-ph/0205241; P. Creminelli *et al.*, arXiv:hep-ph/0102234.

[25] For a recent review on $0\nu\beta\beta$ decay, see S. R. Elliot and P. Vogel, arXiv:hep-ph/0202264.

[26] V. Barger *et al.*, arXiv:hep-ph/0205290.

[27] See P. C. de Holanda and A. Yu. Smirnov in Ref [24].

[28] See http://map.gsfc.nasa.gov/

[29] See http://astro.estec.esa.nl/SA-general/Projects/Planck/.

[30] W. Hu, D. J. Eisenstein and M. Tegmark, Phys. Rev. Lett. **80**, 5255 (1998); M. Tegmark, M. Zaldarriaga and A. J. Hamilton, Nucl. Phys. Proc. Suppl. **91**, 38 (2001).

[31] T. Totani, Phys. Rev. Lett. **80**, 2039 (1998); J. F. Beacom, R. N. Boyd and A. Mezzacappa, Phys. Rev. Lett. **85**, 3568 (2000).
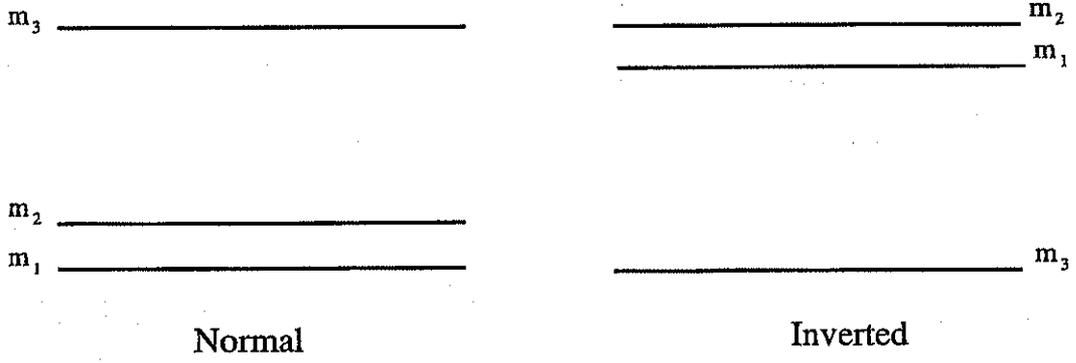
FIG. 1: Mass ordering considered in this work.
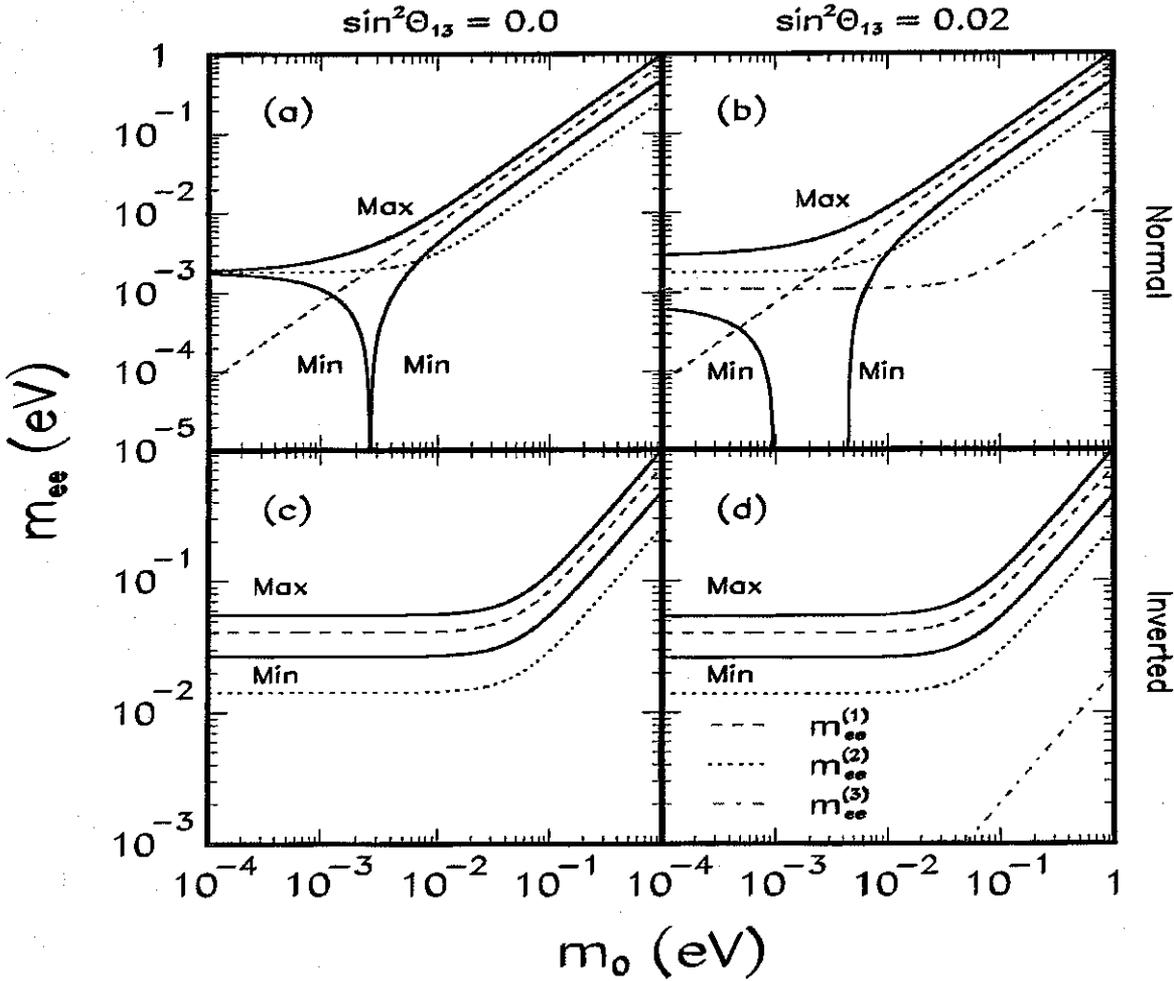
FIG. 2: Maximum and minimum possible values of m_{ee} as a function of m_0 indicated by the thick solid curves for $\sin^2 \theta_{13} = 0$ (left panels) and 0.02 (right panels) for normal (upper panels) as well as for inverted (lower panels) mass ordering. We have fixed the other mixing parameters as $\Delta m_{12}^2 = 5 \times 10^{-5}$ eV^2, $\tan^2 \theta_{12} = 0.35$ and $|\Delta m_{23}^2| = 3 \times 10^{-3}$ eV^2. The individual contributions of $m_{ee}^{(1)}$, $m_{ee}^{(2)}$ and $m_{ee}^{(3)}$ are also shown by dashed, dotted and dash-dotted curves, respectively.

18
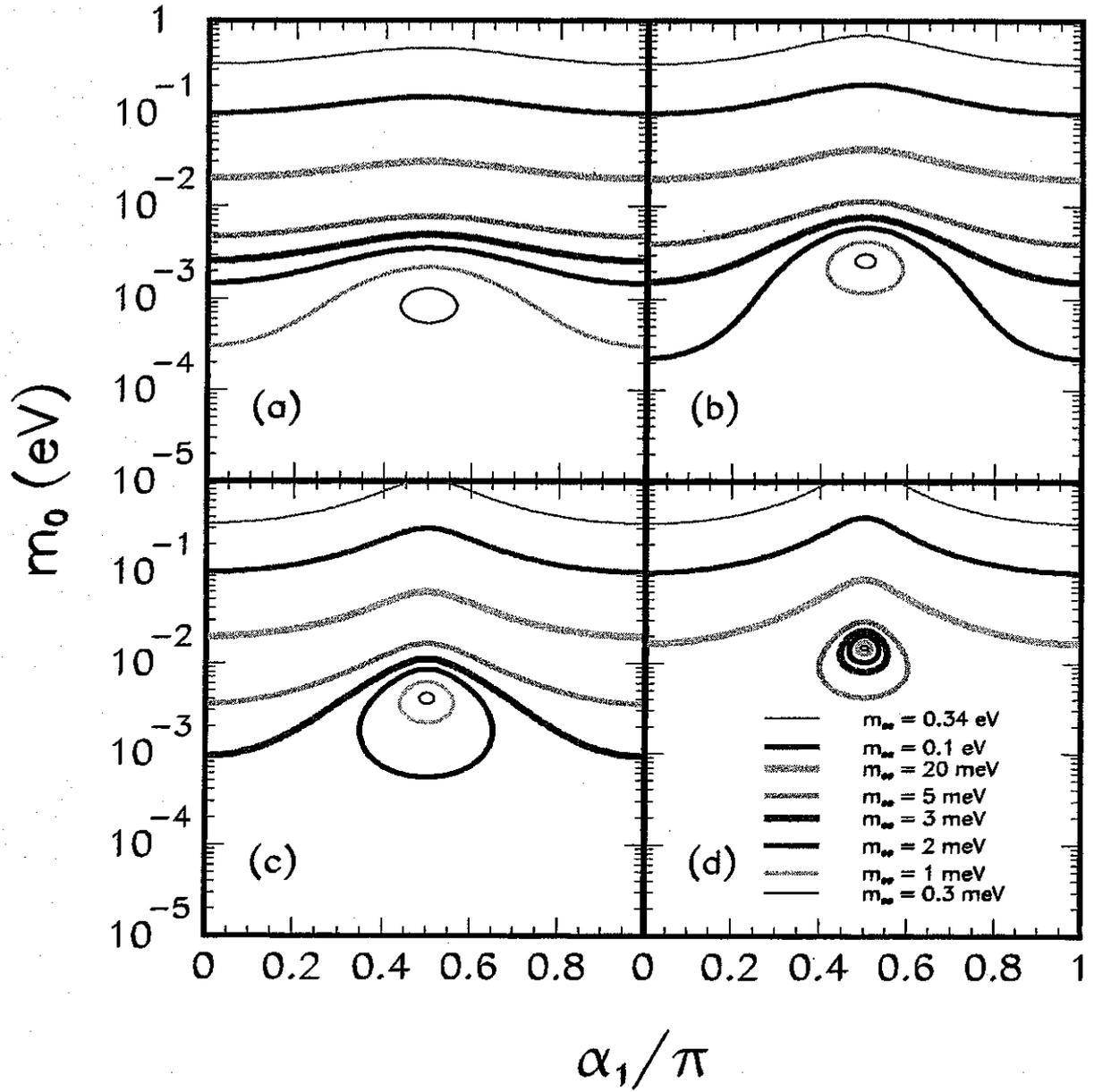
FIG. 3: Iso-contour plots of m_{ee} for $\sin^2 \theta_{13} = 0$ for the normal mass ordering in the $\alpha_1 - m_0$ plane. We have fixed the other relevant mixing parameters as $(\Delta m_{12}^2, \tan^2 \theta_{12}) = (2 \times 10^{-5} \text{ eV}^2, 0.2)$ in (a), $(5 \times 10^{-5} \text{ eV}^2, 0.35)$ in (b), $(5 \times 10^{-5} \text{ eV}^2, 0.5)$ in (c) and $(4 \times 10^{-5} \text{ eV}^2, 0.6)$ in (d).
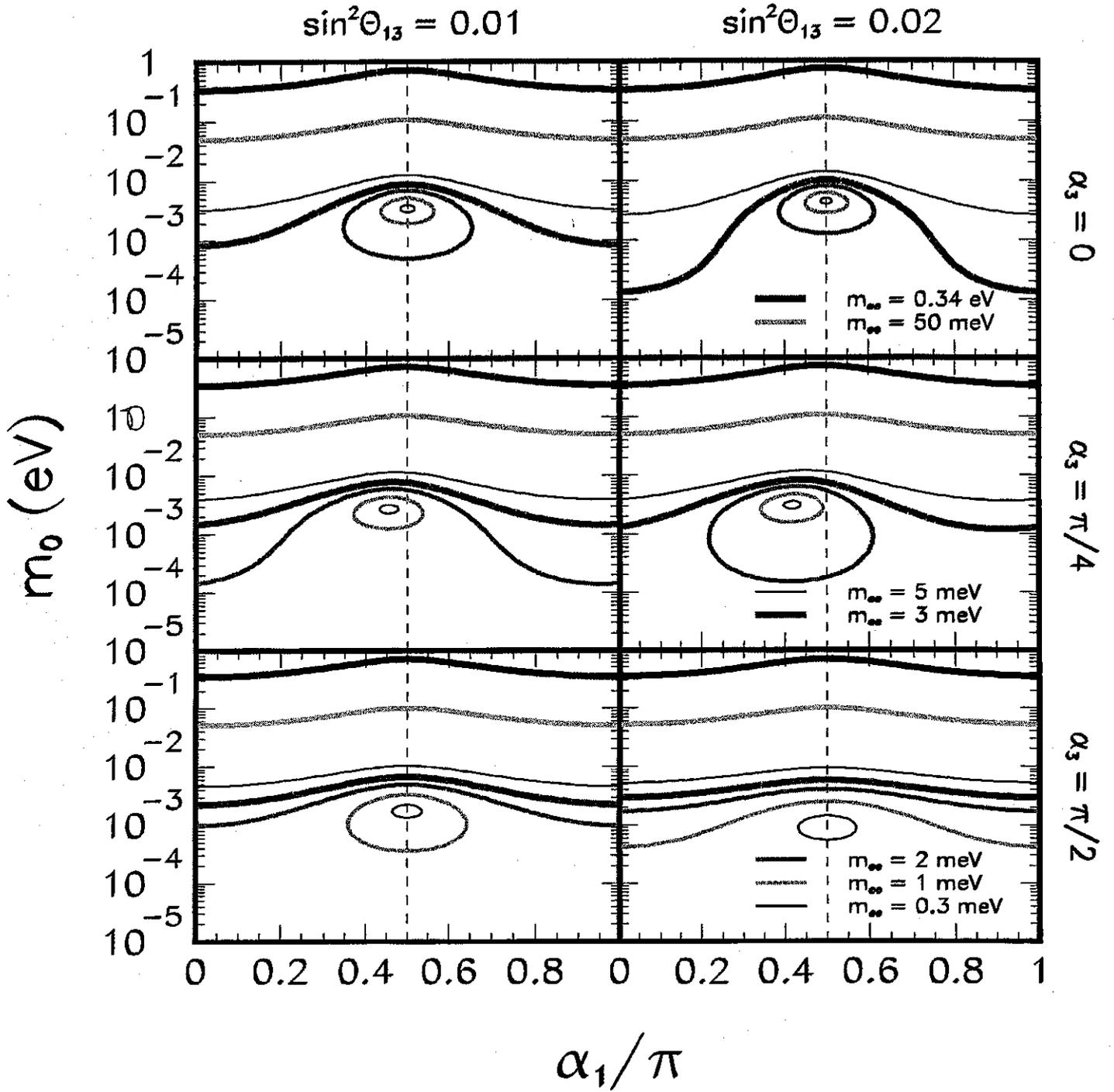
FIG. 4: Same as Fig. 3(b) but for $\sin^2 \theta_{13} = 0.01$ (left panels) and 0.02 (right panels), for $\alpha_3 = 0$ (upper panels), $\pi/4$ (middle panels) and $\pi/2$ (lower panels). The dashed vertical lines mark $\alpha_1/\pi = 0.5$.
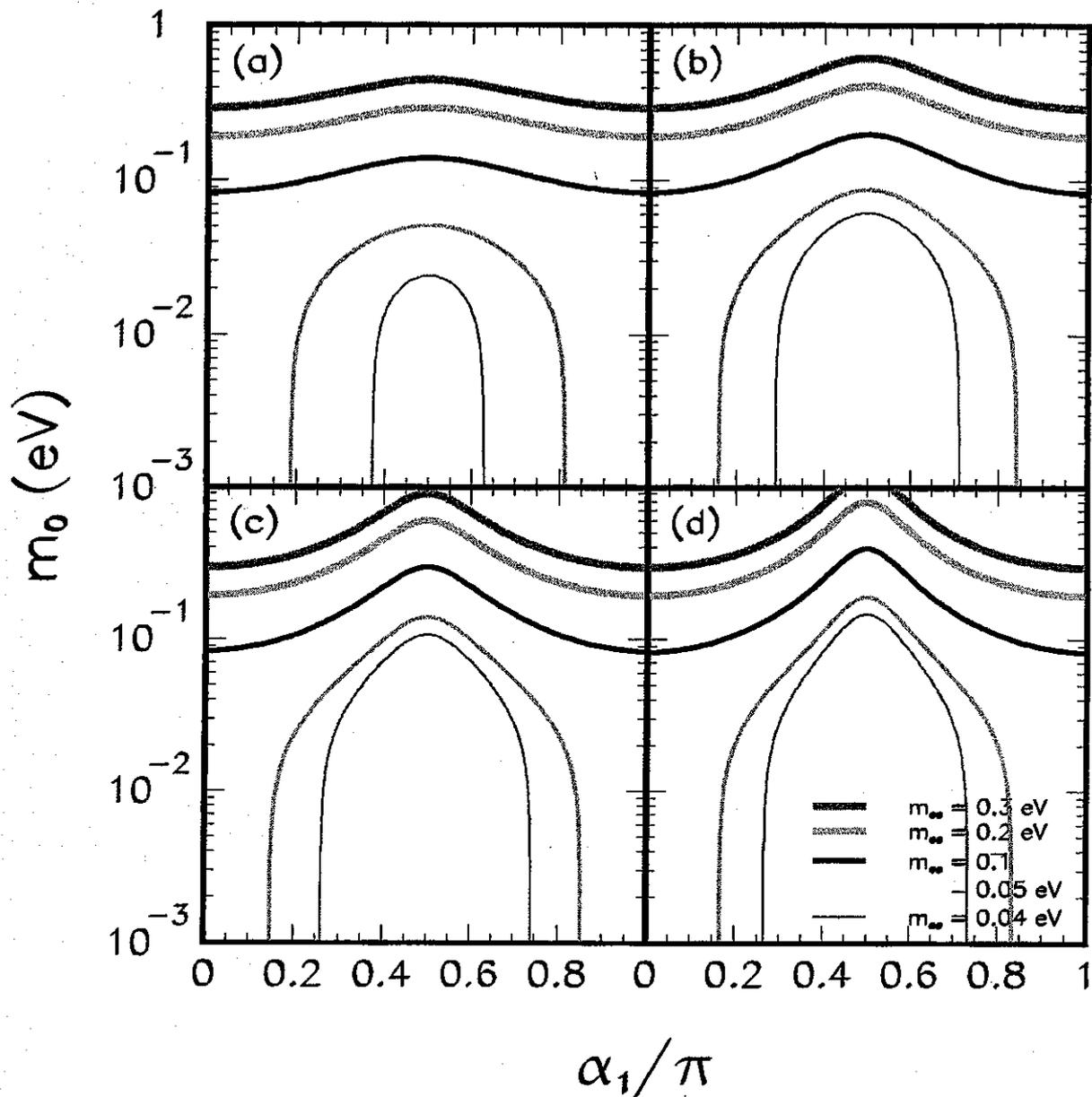
FIG. 5: Same as Fig. 3 but for the inverted mass ordering. Here we have fixed the atmospheric mass scale to $\Delta m^2_{23} = -5 \times 10^{-3}$ eV^2 in (a), to $\Delta m^2_{23} = -3 \times 10^{-3}$ eV^2 in (b) and (c) and to $\Delta m^2_{23} = -1.3 \times 10^{-3}$ eV^2 in (d).
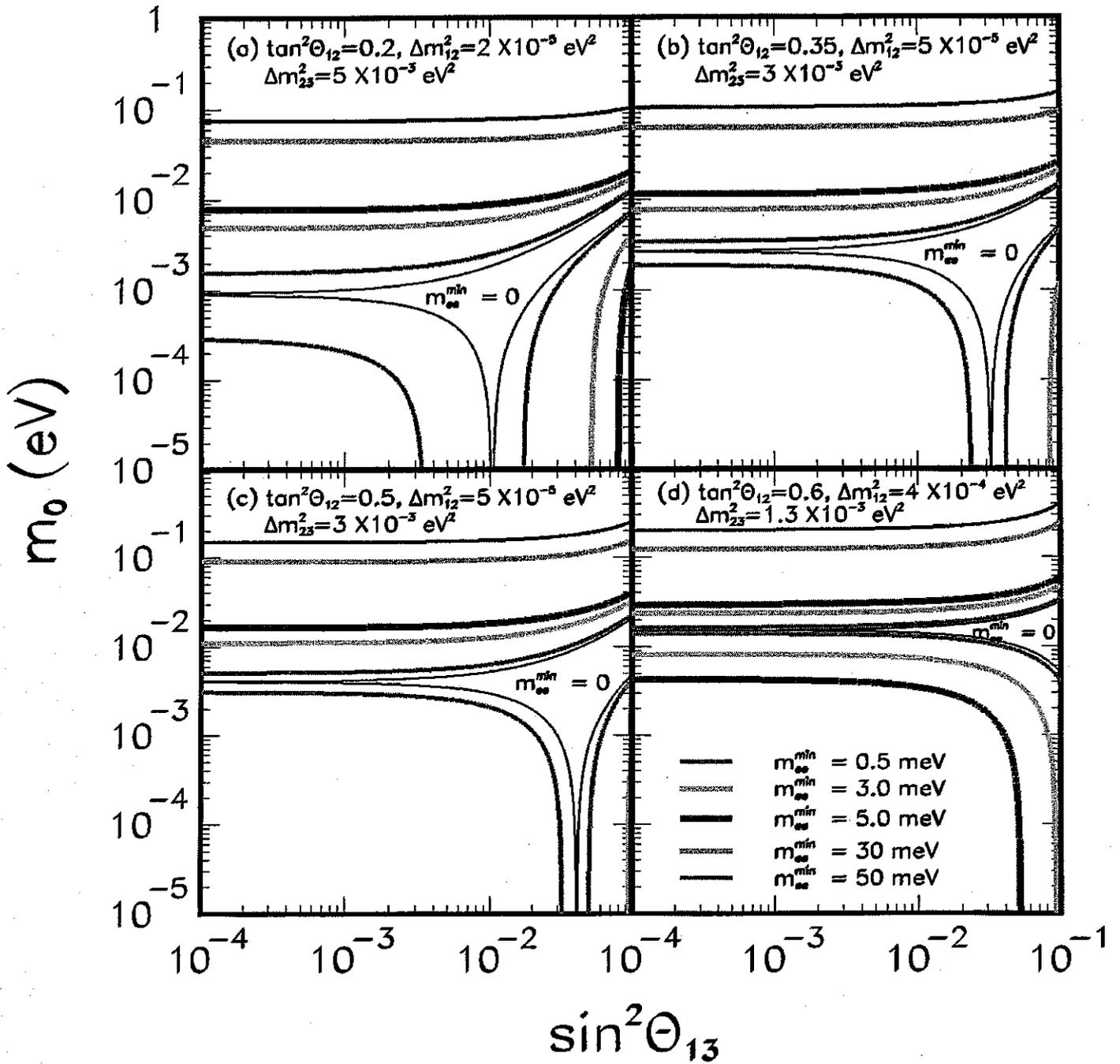
FIG. 6: Iso-contour plots of $m_{ee}^{\min}$ in the $s_{13}^2 - m_0$ plane for different choices of the mixing parameters for the normal mass ordering. We note that in the region delimited by thin solid curves $m_{ee}^{\min} = 0$.
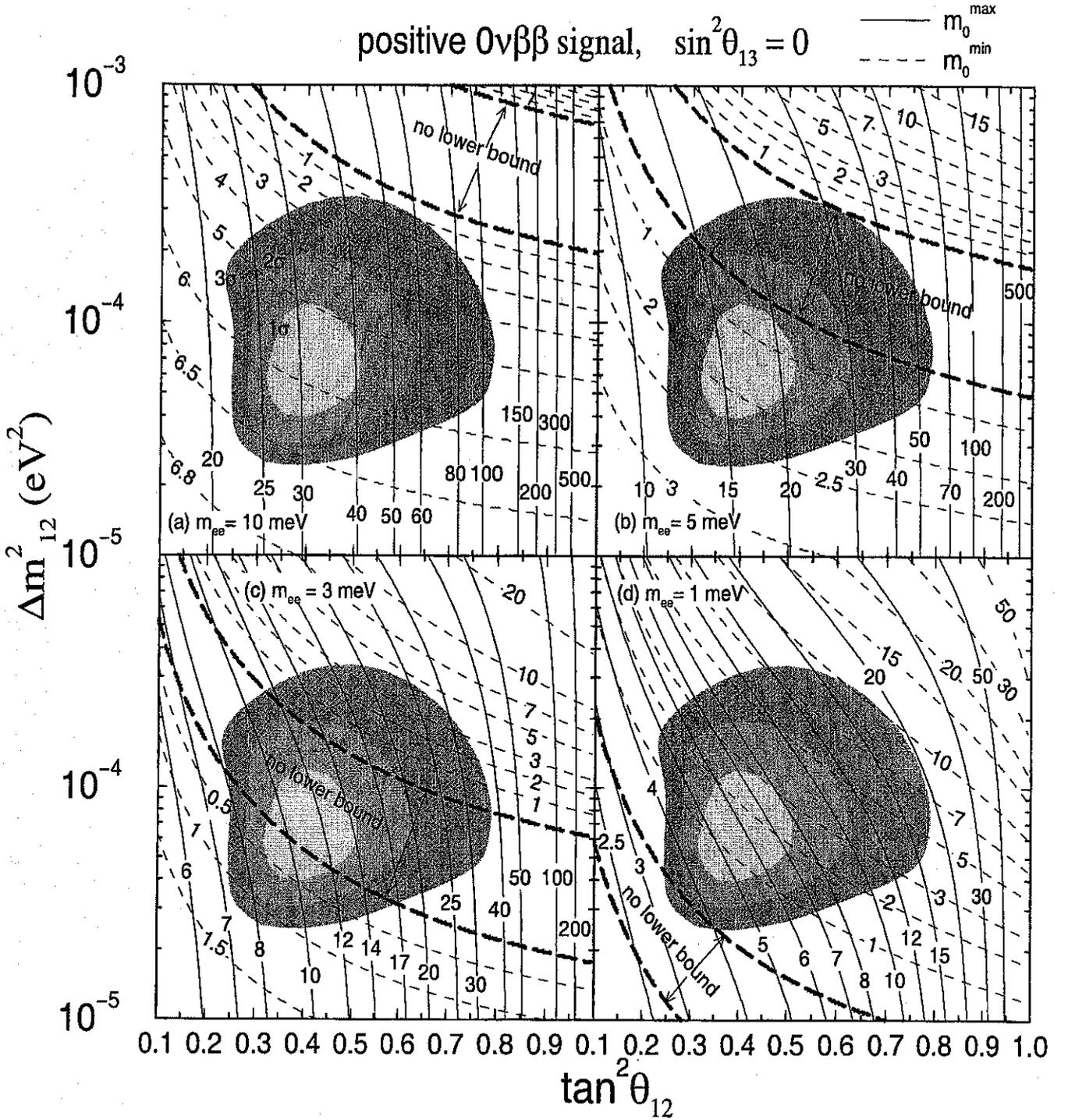
FIG. 7: Iso-contour plots of upper (m_0^{max}, solid curves) and lower (m_0^{min}, dashed curves) bounds of m_0 in units of meV in the $\tan^2 \theta_{12} - \Delta m_{12}^2$ plane for the case where a positive signal of $0\nu\beta\beta$ is observed with central values, $m_{ee} = 10$ meV (a), 5 meV (b), 3 meV (c) and 1 meV (d). We assume 30% uncertainty in the determination of m_{ee}. We fix the other mixing parameters as $\Delta m_{23}^2 = 3 \times 10^{-3}$ eV^2 and $\sin^2 \theta_{13} = 0$. The allowed region for the LMA MSW solution at 1, 2 and 3 σ are shown by the shaded area (adopted from Ref. [27]).
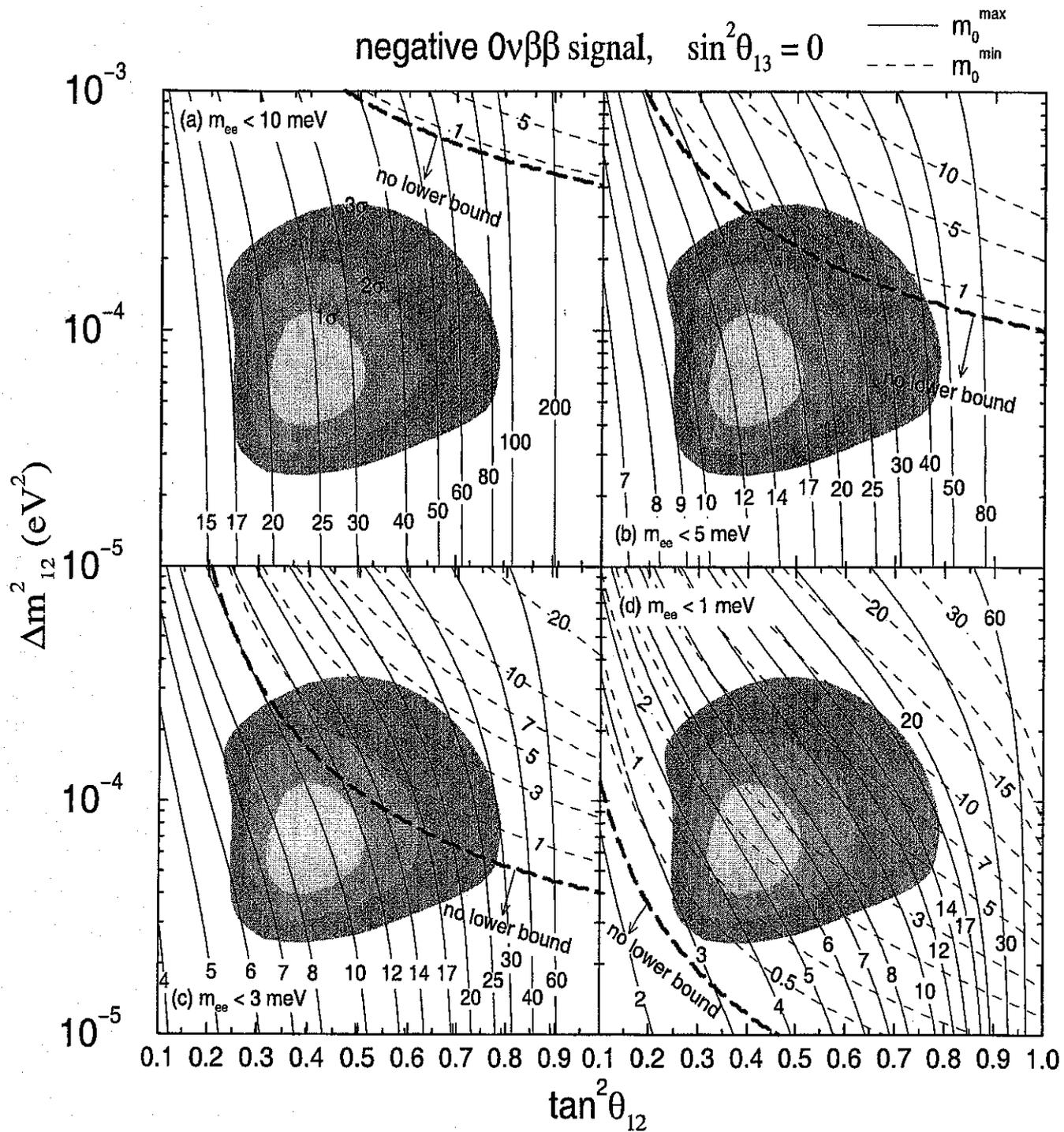
FIG. 8: Same as Fig. 7 but for $\sin^2 \theta_{13} = 0.02$.

FIG. 9: Same as Fig. 7 but for the case where no positive signal of $0\nu\beta\beta$ is observed down to m_{ee} = 10 meV (a), 5 meV (b), 3 meV (c) and 1 meV (d).
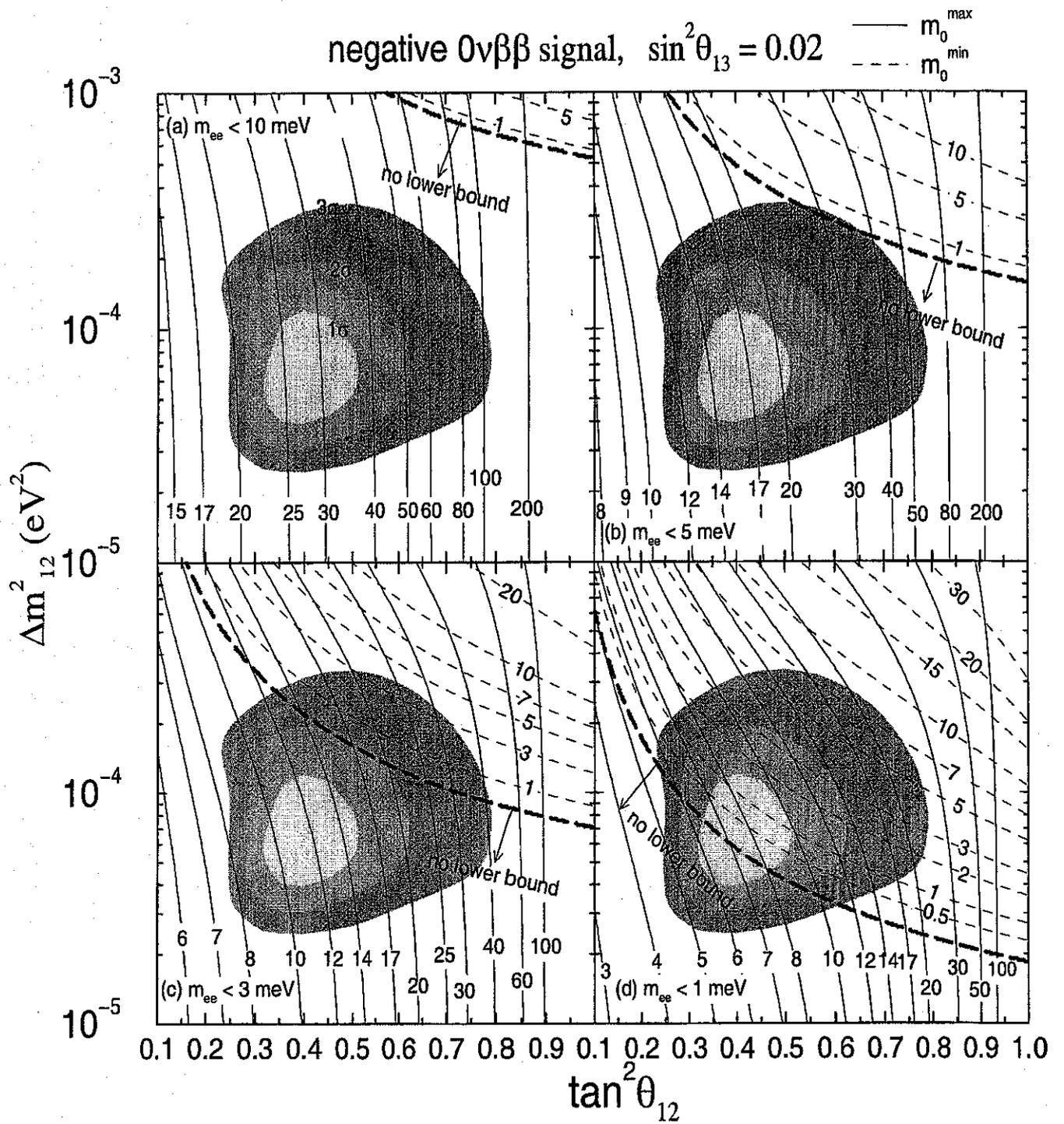
FIG. 10: Same as Fig. 9 but for $\sin^2 \theta_{13} = 0.02$.